Air-to-Ground Channel Modeling for UAV Communications Using 3D Building Footprints

Hajar El Hammouti[1(✉)] and Mounir Ghogho[1,2(✉)]

[1] FIL, TICLab, International University of Rabat, Rabat, Morocco
{hajar.elhammouti,mounir.ghogho}@uir.ac.ma
[2] School of IEEE, University of Leeds, Leeds, UK

Abstract. Unmanned aerial vehicles (UAV) deployment and emerging air-to-ground wireless services have been a topic of great interest in the last few years. The main virtue of UAV networks is that they provide on demand connectivity. However, the design of such networks is intrinsically dependent on the air-to-ground propagation conditions. In order to construct a reliable air-to-ground channel model that takes into account the nature of the surrounding environment, we propose to exploit the information provided by building footprints. The obtained results are compared with existing statistical air-to-ground channel models. It is shown that both the the path loss exponent and the variance of the shadow fading are dependent on the distance on the ground between the UAV and the user and the drone's altitude. The proposed channel modeling method is then used to estimate the coverage probability over the studied area.

Keywords: UAV · Air-to-ground channel · Real building footprints
Shadowing · Coverage probability · Meta-distribution of SNR

1 Introduction

In the last few years, unmanned aerial vehicles (UAV) have gained interest among industrial and research communities as a rapidly deployable network that provides on-demand connectivity. By contrast to terrestrial infrastructures, both expensive and time-consuming in terms of deployment, UAV can be seen as a rapid and efficient support for a short-fall in network capacity after a natural disaster or during a temporary mass event. Additionally, in the wide Internet of things (IoT) ecosystem, UAV can also be used as mobile base stations that move towards IoT devices, provide connectivity, collect and relay data to terrestrial gateways or out-of-range receivers.

While UAV networks use cases are numerous [14], their deployment, however, is associated with several technical challenges that need to be addressed. Many issues related to network architecture [7], energy consumption [16], interference management [18,19], coverage and movement optimization [12,15], and

N. Boudriga et al. (Eds.): UNet 2018, LNCS 11277, pp. 372–383, 2018.
https://doi.org/10.1007/978-3-030-02849-7_33

air-to-ground channel modeling [2] have been presented in the literature. These challenges, commonly discussed for ground-to-ground communications, need to be addressed from an air-to-ground communication perspective. This is because the air-to ground propagation conditions are different from the terrestrial ones. For example, a drone's coverage is tightly related to its position, in particular its altitude. Indeed, improving a drone's altitude has a double-edged sword effect: it provides a stronger link with a higher probability of line-of-sight, but at the same time, it results in an important path loss. This tradeoff has been the subject of many research papers that aim to optimize the drone's altitude while maximizing its coverage. In [15], authors show the concavity of the coverage probability with respect to a single drone's altitude. In [10], authors investigate the optimal altitude by taking into account different antenna's gain patterns and a multi-path fading channel. Interference is considered in [18] where the authors derive the probability of coverage using a dominant interferer approach. Additional interferences, resulting from coexistence with device-to-device communications (D2D), are characterized in [17] which provides a closed-form expression of the coverage probability.

Despite the large amount of existing works that address UAV coverage from a theoretical perspective, the experimental validation of these results is still in its infancy. In general, the air-to-ground channel is represented by an average path loss model obtained by assuming both LOS and non-LOS links [4,5,11]. Although this statistical model provides a good baseline for the network performance on average, it may not predict accurately the coverage for a *specific* urban area. Alternatively, the radio channel can be estimated with high precision using ray-tracing softwares. However, the problem with ray-tracing is that it involves expensive softwares requiring very high load and execution time as well as very accurate 3D map of the urban area including type of building materials. The idea behind our work is to propose a hybrid approach that uses the 3D buildings footprints to estimate the shadowing component, and employs statistical models for the small-scale fading. The proposed channel modeling is then used to estimate the coverage probability as a function of the UAV's position. In this paper, the 3D building footprints from Paris city is used as a use case.

The contributions and organization of the paper are as follows.

1. A comprehensive description of the system model, the studied area, and the realistic channel model that takes into account buildings blockages is provided (see Sect. 2).
2. A simplified method to determine the channel models in terms of LOS probability, and shadowing mean and variance, by using real building footprints is proposed. Our results show that the path loss exponent and the shadowing variance are dependent on both the UAV altitude and the distance on the ground between the UAV and the user (see Sect. 3).
3. To evaluate the coverage, two performance metrics are considered: coverage probability and the meta-distribution of signal-to-noise-ratio (SNR) (see Sect. 4).

4. Simulation results that estimate the coverage probability are discussed (see Sect. 5), and concluding remarks are provided (see Sect. 6).

2 System Model

In this section, we present the studied area and explain the data extraction process. We also provide a comprehensive description of the adopted air-to-ground channel model.

2.1 Area Under Study

In order to capture the effect of buildings obstructions, we consider an urban area from the 16$^{\text{ème}}$ arrondissement of Paris. Specifically, we are interested in an area $\mathcal{A}$ of 1055×990 m^2 located at the eastern part of the district as described in Fig. 1. In addition of being a prestigious residential neighborhood, the area of study hosts a large number of companies (PSA Peugeot Citroen, Lafarge ..) and includes a concentration of museums and touristic sites (Guimet museum, Trocadéro place ..) which makes it an interesting case of study (as a dense and diverse area). Data related to area $\mathcal{A}$ is available in [1]. It mainly contains buildings footprints that describe the buildings shapes in 2D (in a shape file) and the number of levels per building (in an excel file) of all Paris city. Since the exact heights of the buildings are not provided, we use, instead, the number of levels per building times the average height per level (2.9 m for Paris). Even though this approximation is not perfectly accurate, it provides good insights on the impact of buildings elevation on coverage. A summary of the characteristics of the studied area is given in Table 1.

(a) (b)

Fig. 1. A Google map view of the 16$^{\text{ème}}$ arrondissement with a highlight on the studied area, (b) The entire area under analysis with base stations locations, x and y axis express distances in meters

Table 1. A summary of the region under analysis

Location	Area (m × m)	Center location (longitude, latitude)	Density of Buildings	Average number of levels
Paris (16ème)	1055 × 990	(2.27978, 48.86185)	47%	4.13

To extract desirable data from raw data provided by [1], we proceed as follows.

1. A master file that contains all the building footprints of Paris city is downloaded from [1].
2. Data related to the studied area are extracted using Quantum Geographic Information System software (QGIS) [13]. The resulted file is uploaded to Matlab using the mapping toolbox.
3. Users positions are generated in the 2D plane according to a circular grid. The choice of the circular grid provides an easy way for probability of line of sight computation (more details are provided in Sect. 3.1).
4. For the sake of comparison with existing statistical models that assume outdoor users, we remove all points inside building polygons.
5. The UAV is located at the center of the area with fixed x_0 and y_0 coordinates, and a variable altitude h.

2.2 Blockage Model

In an urban type environment, the distortion of the signal due to shadowing is intrinsically dependent on the number of buildings between the UAV and the ground user. In order to capture the effect of obstructions caused by buildings, we adopt the shadowing model proposed in [6].

Assume that N_i is the number of intersected buildings between user i and the UAV. To reach the user, the transmitted signal has to penetrate N_i buildings that cause, for each, a propagation loss of K_b, where $K_b \in [0, 1]$ is the penetration loss related to building b. For the sake of simplicity, we assume that $K_b = K$ is the same for all buildings. As a consequence, the shadowing attenuation h_i between user i and the UAV is given by

$$\zeta_i = K^{N_i}. \tag{1}$$

Note that, when no shadowing is considered, i.e. there is a line-of-sight between the UAV and the ground user, $N_i = 0$ and thus $\zeta_i = 1$.

2.3 Free Space Path Loss Model

We use the standard power-law path loss model where the path loss attenuation between user i and the UAV separated by distance $(r_i^2 + h^2)^2$ is given by $(r_i^2 + h^2)^{\frac{-\alpha_1}{2}}$, with α_1 being the path loss exponent, and r_i is the distance between user i and the projection of the UAV on the 2D plane.

2.4 Small-Scale Fading

We adopt the commonly used Rayleigh fading. We also assume that the Rayleigh channel gains are independent and identically distributed (i.i.d). Hence, the channel power gain g_i between user i and the UAV is a random variable that follows a standard exponential distribution.

3 Simplified Air-To-Ground Channel Model

In this section, we provide a general method to evaluate LOS probability and shadowing mean and variance by using real 3D building footprints.

3.1 Line of Sight Probability

The probability of LOS is a key element when modeling the air-to-ground channel. It is particularly useful to identify straight paths between the UAV and the ground user. In order to compute such probability, we generate outdoor users according to a circular grid centered on the projected position of the UAV on the ground (x_0, y_0). For each circle $\mathcal{C}_j(x_0, y_0, r_j)$ of radius r_j, we identify the number of outdoor users that have a LOS with the UAV. The probability of LOS at a radius $r = r_j$ and an altitude h is estimated as the percentage of outdoor users on the circle that have a LOS with UAV.

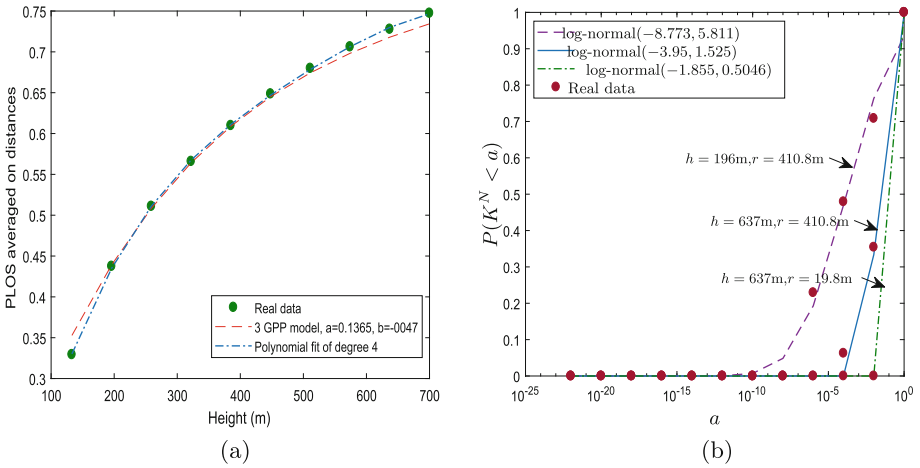

Fig. 2. (a) Average LOS probability, (b) Cumulative distribution function of shadowing, $K = -20\,\text{dB}$

In Fig. 2(a), we compare the actual LOS probability with the following existing statistical model [15]

$$p_{LOS}(r,h) = \frac{1}{1 + a\exp\left(-b(\frac{180}{\pi}arctan\frac{r}{h} - a)\right)} \tag{2}$$

where the environmental-dependent variables a and b are obtained by performing a non-linear least square data fitting.

Figure 2(a) plots the probability of LOS as a function of the UAV's altitude. These results are obtained by averaging over 100 distances. We observe a good agreement between the fit of the statistical model and actual data ($R^2 = 0.88$). This fit can be slightly improved by using a polynomial function of degree 4 ($R^2 = 0.9$). As intuitively expected, the probability of LOS is improved when the drone increases its altitude. This is justified by a significant reduction of intersected buildings as the UAV moves up.

3.2 Shadowing

The shadowing accounts for random losses caused by obstructions along the propagation link. In general, the random behavior of shadow fading is modeled by a log-normal variable, with constant mean and variance, that reflects the multiplicative penetration loss caused by buildings [8].

Shadowing CDF. In Fig. 2(a), the cumulative distribution function (CDF) of the adopted shadowing model is plotted. As depicted in the figure, the actual model is compatible with the log-normal shadowing widely adopted in the literature. However, these observations show that the parameters of the log-normal fading are both distance and altitude-dependent. This is corroborated by the next findings regarding the mean and variance of the adopted shadowing model.

Shadowing Mean. To study the shadowing distribution caused by buildings, a good understanding of the mean and variance structure is required. In fact, the shadowing mean with respect to the distance r and height h, $\mu(r,h)$, can be written

$$\mu(r,h) = \sum_{n=0}^{+\infty} \mathbb{P}(N_i(r,h) = n)K^n, \tag{3}$$

where $N_i(r,h)$ denotes the number of intersected buildings for a given distance r and altitude h, and $\mathbb{P}(N_i(r,h) = n)$ is the probability that n buildings are intersected at distance r and altitude h.

The shadowing mean for $r = 311.85$ is plotted in Fig. 3(a). As shown in the figure, the mean value increases with altitude. Moreover, it can be noticed from the same figure that the shadowing mean can be approximated, with a good fit, by a power law function. The shadowing mean is therefore estimated as follows

$$\mu(r,h) \approx (r^2 + h^2)^{-\alpha_2(r,h)/2}. \tag{4}$$

In Fig. 3(b), we plot an approximation of $\alpha_2(r, h)$ for the same distance ($r = 311.85\,\text{m}$) versus the UAV's height. α_2 is then estimated as follows

$$\alpha_2(r, h) = a_0 r^{b_0} h^{-c_0} - d_0 h + e_0, \tag{5}$$

where a_0, b_0, c_0, d_0 are a non negative parameters to be determined, with the parameter e_0, through curve-fitting.

The proposed fit provides a good estimation of real data, the resulted $R^2 = 0.93, 0.9, 0.88$ for $K = -3\,\text{dB}$, $-10\,\text{dB}$, $-20\,\text{dB}$ respectively. Moreover, it can be noticed from Eq. (5) and Fig. 3(b) that the shadowing mean exponent, α_2, decays with the drone's height. This is attributed to the fact that the number of intersected buildings decreases as the UAV moves up. These findings are in line with conclusions of works in [20] and [3] where authors show that the path loss exponent decreases with altitude. On the other side, α_2 increases with distance as additional penetration loss will be accumulated for an increasing distance (and fixed height).

Another more intuitive finding is that the shadowing mean estimation is tightly related to buildings penetration loss. In particular the shadow mean increases as the penetration loss increases. This is intuitively expected as additional penetration loss will result in higher shadowing values.

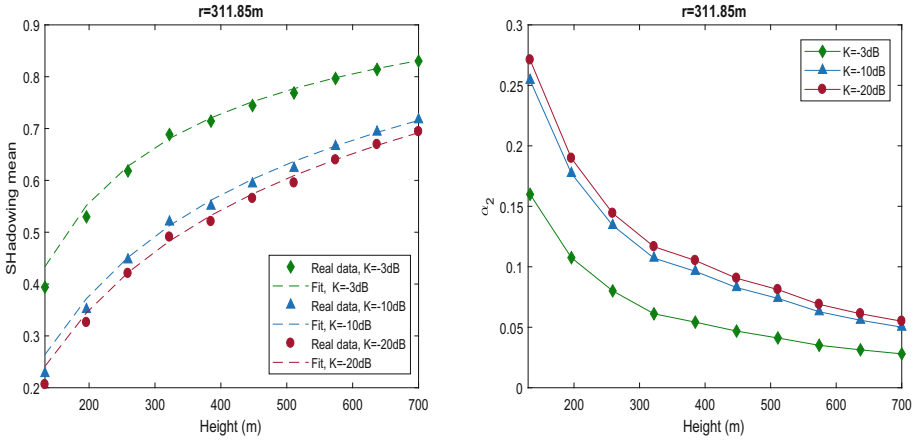

Fig. 3. (a) The mean of the shadowing for distance $r = 361.35\,\text{m}$, (b) Exponent of the shadowing mean $r = 311.85\,\text{m}$

Shadowing Variance. The results in Fig. 4(a) show the height-dependency of the shadowing variations for $r = 311.85\,\text{m}$. In fact, the estimated variance increases as the UAV improves its altitude until a maximal value before it decreases with height. The existence of a height that maximizes the variance

depends on the penetration loss. Indeed, when the penetration loss is low, the shadowing variance monotonically decreases with height. Furthermore, the figure shows that the shadowing variance is reduced when the penetration loss is lower. This is attributed to the fact that a building with a lower penetration loss will cause a lower signal distortion. The figure proposes also a simplified expression to estimate the variance by using the following polynomial fit

$$\sigma^2(r,h) \approx \sum_{i=0}^{i=4} \sum_{j=0}^{j=4} a_{ij} r^i h^j, \tag{6}$$

where a_{ij} are determined through curve-fitting. The proposed variance fit results in $R^2 = 0.86, 0.75, 0.75$ for $K = -3\,\text{dB}, -10\,\text{dB}, -20\,\text{dB}$ respectively.

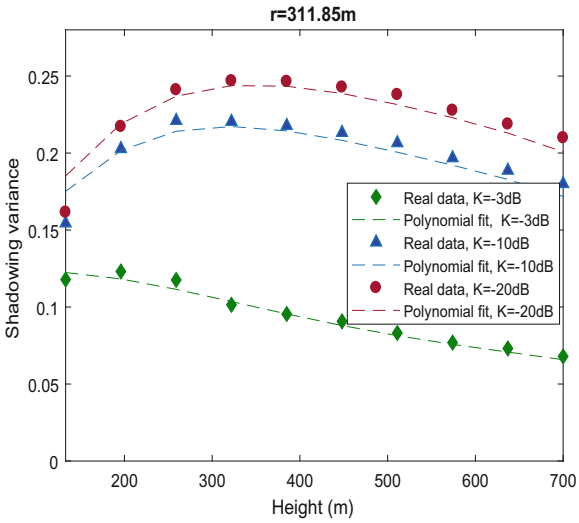

Fig. 4. Variance of the shadowing for distance $r = 311.85\,\text{m}$

It is worth mentioning that the proposed simplified shadowing model does not include correlation. An accurate model should capture spatial correlation between neighboring users. This has been left as part of future work.

4 Performance Metrics

In order to evaluate the effects of shadowing on coverage, we consider two performance metrics: average coverage probability and the meta-distribution of SNR.

4.1 Average Coverage Probability

We consider downlink communication. Hence, when a frame is transmitted by the UAV with power P, it is received at the ground user t with the power $Pg_tK_t^N(r_t^2+h^2)^{-\alpha_1}$. The quality of the wireless link is measured in terms of SNR γ_t, which is defined as

$$\gamma_t = \frac{Pg_tK_t^N(r_t^2+h^2)^{-\alpha_1}}{\sigma^2}, \tag{7}$$

where σ^2 represents the power of an additive Gaussian noise.

We are interested in coverage probability for a given user t, which is the probability that the SNR of that user is above a given threshold θ. This probability can also be seen as the complementary cumulative distribution function (CCDF) of the user's SNR and can be written as

$$P_c(t;\theta) = \mathbb{P}(\gamma_t > \theta), \tag{8}$$

Note that this probability is calculated over small-scale fading.

In order to evaluate the general behavior of coverage, we average the coverage probability over the user's positions. The resulting average coverage probability is defined as

$$\tilde{P}_c(\theta) = \frac{1}{|\mathcal{A}|}\int_{\mathcal{A}} \mathbb{P}(\gamma(t) > \theta)dt, \tag{9}$$

with $|\mathcal{A}|$ the surface of the studied area $\mathcal{A}$, and $\gamma(t)$ is the SNR of a ground user at position t. For simulations, the integral in Eq. (9) is computed numerically by considering a finite number of user's positions (2890 positions in our case).

4.2 Meta-Distribution of SNR

The meta-distribution of SNR provides a better information about the performance of the coverage probability. It answers the question 'to what extend the coverage is good?' [9]. For a given threshold θ, and a fixed position of UAV, the meta-distribution is given by the percentage of users that achieve a coverage performance higher than a threshold x. This can be formulated as follows

$$P_m(x,\theta) = \mathbb{P}(P_c(t;\theta) > x), \tag{10}$$

with $x \in [0,1]$.

5 Coverage Experiments

In this section, we present simulation experiments for coverage performance. Details about simulation settings are provided in Table 2.

Figure 5(a) shows the average coverage probability versus the UAV altitude. Here, it can be seen that for a given desired coverage, there exists an optimal

Table 2. Simulation settings

Parameter	Value
Number of user positions	2890
Monte Carlo simulations	1000
Path loss exponent	$\{2, 3.4\}$
Noise power	-100 dBm
BS power	1 mW
Penetration loss	$\{-20, -10, -3\}$ dB
Small-scale fading	Rayleigh with parameter 1

altitude at which the average coverage is at its maximum. This optimal altitude is achieved at 700 m when the path loss exponent $\alpha_1 = 2$, and is equal to 448 m for $\alpha_1 = 3.4$. Furthermore, the results show that the average coverage probability can be predicted approximately using statistical fits (provided in Sect. 3). The accuracy of such approximation could be improved when spatial correlation is included in the shadowing modeling. In Fig. 5(b), the average meta-distribution

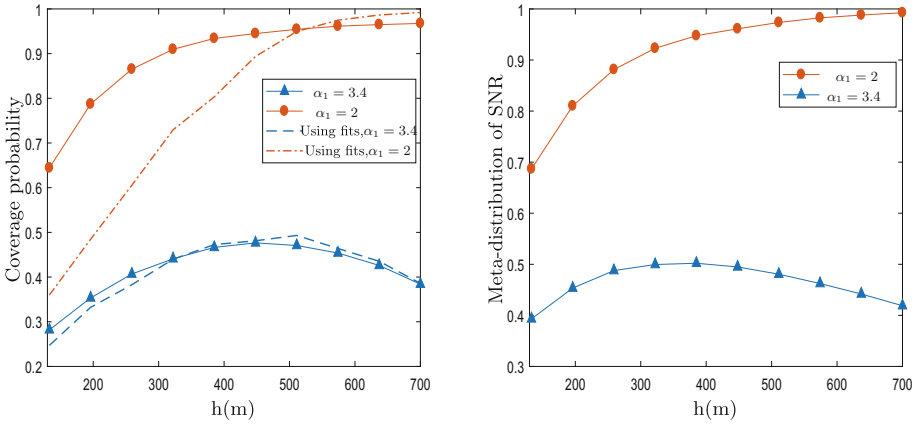

Fig. 5. (a) Average coverage probability, (b) Average of the meta-distribution of coverage. $K = -20$ dB, $\theta = -20$ dB.

of SNR (average on θ and x) is plotted versus the drone's altitude. Once again, we observe the same trend as for the coverage probability. Moreover, it can be noticed from Fig. 6 that the meta-distribution of SNR decreases when the thresholds θ and x increase as intuitively expected.

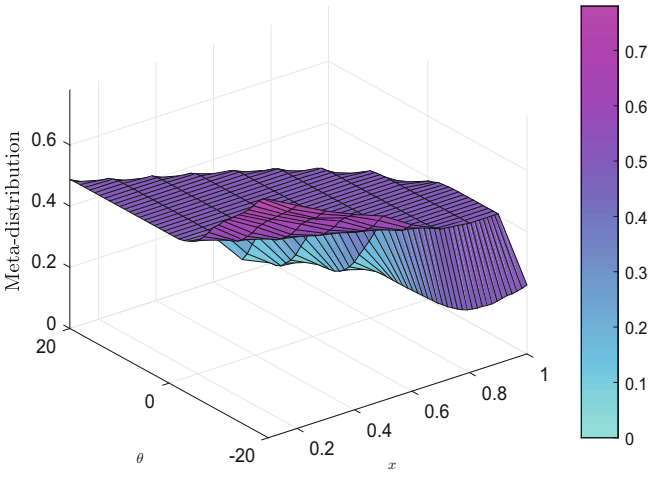

Fig. 6. A 3D illustration of the meta-distribution, $h = 322\,\mathrm{m}$, $K = -20\,\mathrm{dB}$

6 Conclusion

In this paper, we presented a general framework to model the air-to-ground channel model using 3D building footprints. More specifically, we proposed to use 3D building maps to estimate the line-of-sight probability, the CDF of the shadowing and its mean and variance. Our findings show that it is important to include distance and altitude-dependent parameters for the air-to-ground channel modeling. Particularly, we showed that the path loss exponent decreases with UAV's altitude and increases with the distance on the ground between the UAV and the user. We also showed that the shadow fading variance is reduced for higher altitudes. Furthermore, our proposed method allows for a tractable way of estimating the wireless coverage of urban areas. Indeed, instead of using sophisticated ray-tracing techniques that are both expensive and time-consuming, only 3D maps are needed in order to provide a reliable channel modeling. In ongoing work, we are investigating the effect of the spatial shadow correlation, and interfering UAVs on coverage performance.

References

1. https://opendata.paris.fr/explore/dataset/volumesbatisparis2011/ (2017)
2. Al-Hourani, A., Kandeepan, S., Jamalipour, A.: Modeling air-to-ground path loss for low altitude platforms in urban environments. In: IEEE Global Communications Conference (GLOBECOM), Austin, USA, pp. 2898–2904, December 2014
3. Amorim, R., Nguyen, H., Mogensen, P., Kovács, I.Z., Wigard, J., Sørensen, T.B.: Radio channel modeling for UAV communication over cellular networks. IEEE Wirel. Commun. Lett. **6**(4), 514–517 (2017)

4. Azari, M.M., Murillo, Y., Amin, O., Rosas, F., Alouini, M.S., Pollin, S.: Coverage maximization for a poisson field of drone cells. arXiv preprint arXiv:1708.06598 (2017)
5. Azari, M.M., Rosas, F., Chiumento, A., Pollin, S.: Coexistence of terrestrial and aerial users in cellular networks. arXiv preprint arXiv:1710.03103 (2017)
6. Baccelli, F., Zhang, X.: A correlated shadowing model for urban wireless networks. In: 2015 IEEE Conference on Computer Communications (INFOCOM), pp. 801–809 (2015)
7. Bucaille, I., Héthuin, S., Munari, A., Hermenier, R., Rasheed, T., Allsopp, S.: Rapidly deployable network for tactical applications: aerial base station with opportunistic links for unattended and temporary events absolute example. In: IEEE Military Communications Conference (MILCOM), San Diego, USA, pp. 1116–1120, November 2013
8. Coulson, A.J., Williamson, A.G., Vaughan, R.G.: A statistical basis for lognormal shadowing effects in multipath fading channels. IEEE Trans. Commun. **46**(4), 494–502 (1998)
9. Haenggi, M.: The meta distribution of the SIR in poisson bipolar and cellular networks. IEEE Trans. Wirel. Commun. **15**(4), 2577–2589 (2016)
10. Hayajneh, A.M., Zaidi, S.A.R., McLernon, D.C., Ghogho, M.: Optimal dimensioning and performance analysis of drone-based wireless communications. In: IEEE Globecom Workshops (GC Wkshps), pp. 1–6 (2016)
11. Kalantari, E., Yanikomeroglu, H., Yongacoglu, A.: On the number and 3D placement of drone base stations in wireless cellular networks. In: IEEE Vehicular Technology Conference (VTC-Fall), pp. 1–6 (2016)
12. Lee, G., Saad, W., Bennis, M., Mehbodniya, A., Adachi, F.: Online ski rental for scheduling self-powered, energy harvesting small base stations. In: IEEE International Conference on Communications (ICC), Kuala Lumpur, Malaysia, pp. 1–6, May 2016
13. Q Software Manual. http://www.qgis.org/en/site/ (2017)
14. Motlagh, N.H., Taleb, T., Arouk, O.: Low-altitude unmanned aerial vehicles-based internet of things services: comprehensive survey and future perspectives. IEEE Internet Things J. **PP**(99), 1–27 (2016)
15. Mozaffari, M., Saad, W., Bennis, M., Debbah, M.: Drone small cells in the clouds: design, deployment and performance analysis. In: IEEE Global Communications Conference (GLOBECOM), San Francesco, USA, pp. 1–6, December 2015
16. Mozaffari, M., Saad, W., Bennis, M., Debbah, M.: Efficient deployment of multiple unmanned aerial vehicles for optimal wireless coverage. arXiv preprint arXiv:1606.01962 (2016)
17. Mozaffari, M., Saad, W., Bennis, M., Debbah, M.: Unmanned aerial vehicle with underlaid device-to-device communications: performance and tradeoffs. IEEE Trans. Wirel. Commun. **15**(6), 3949–3963 (2016)
18. Ravi, V.V.C., Dhillon, H.: Downlink coverage probability in a finite network of unmanned aerial vehicle (UAV) base stations. In: IEEE International Workshop on Signal Processing Advances in Wireless Communications (SPAWC), Edinburgh, United Kingdom, pp. 1–5, July 2016
19. Rohde, S., Wietfeld, C.: Interference aware positioning of aerial relays for cell overload and outage compensation. In: IEEE Vehicular Technology Conference (VTC Fall), Quebec, Canada, pp. 1–5, September 2012
20. Sallouha, H., Azari, M.M., Chiumento, A., Pollin, S.: Aerial anchors positioning for reliable RSS-based outdoor localization in urban environments. IEEE Wirel. Commun. Lett. **PP**(99) (2017)